Journal of Hydraulic Research Vol. 42, No. 3 (2004), pp. 316–322

Drag reduction in skimming flow on stepped spillways by aeration

Réduction du frottement des écoulements écumant sur les seuils en marches d'escalier par aération

H. CHANSON, Reader, *Fluid Mechanics, Hydraulics and Environmental Engineering, Department of Civil Engineering, The University of Queensland, Brisbane QLD 4072, Australia. Fax: (61 7) 33 65 45 99; e-mail: h.chanson@uq.edu.au*

ABSTRACT
In skimming flows on stepped spillway, flow resistance is predominantly a form drag process. Cavity recirculation and air entrainment are intense. The interactions between entrained air bubbles and mixing layers may cause some reduction in flow resistance. The paper presents new evidence showing a reduction in friction factor in skimming flow with increasing free-surface aeration. The experimental data are based upon detailed air–water flow measurements in large size models and may be extended to prototypes. The results might suggest some drag reduction, although comparable clear-water flow data are rare.

RÉSUMÉ
Dans les écoulements écumant sur seuils en marche d'escalier, la résistance à l'écoulement est principalement une résistance de forme. La recirculation en cavite et l'entraînement d'air sont intenses. Les interactions entre les bulles d'air entraînées et les couches de mélange peuvent causer une certaine réduction de résistance à l'écoulement. Cette note présente de nouvelles preuves d'une réduction du facteur de frottement dans l'écoulement écumant avec l'augmentation de l'aération de surface libre. Les données expérimentales sont basées sur des mesures détaillées d'écoulement air–eau dans des modèles de grande taille et peuvent être extrapolées aux prototypes. Les résultats pourraient suggérer une certaine réduction de frottement, bien que les données comparables d'écoulement d'eau claire soient rares.

Keywords: Skimming flow, stepped spillway, flow resistance, drag reduction, air entrainment.

1 Introduction

Stepped spillways have been used for more than 3500 years because of the ease of construction and design simplicity. Since the beginning of the 20th century, stepped chutes have been designed more specifically to dissipate flow energy (e.g. New Croton dam). Recently, new construction materials (e.g. RCC, strengthened gabions) have increased the interest for stepped channels and spillways. The construction of stepped chutes is compatible with the slipforming and placing methods of roller compacted concrete, with the construction techniques of gabion dams and with the precast concrete block system technique (e.g. Peyras *et al*., 1992; Chanson, 2001).

On a given stepped chute, low flows behave as a succession of free-falling nappes while, at large discharges, the water skims over the pseudo-invert formed by the step edges (Fig. 1). The skimming flow regime is characterized by strong, three-dimensional cavity recirculation, and the flow resistance is primarily a form drag process (Rajaratnam 1990; Chanson *et al*., 2000). For the past decades, there have been a debate on flow resistance estimate in skimming flows, with experimental results spreading over three orders of magnitude. Current expertise suggests that the dimensionless friction coefficient (or Darcy friction factor) is about 0.1–0.3 (e.g. Table 1, column 6). However air entrainment is always significant downstream of the inception point and the flow resistance may be affected by some drag reduction induced by free-surface aeration. Recently incomplete evidences of drag reduction were produced independently by Boes (2000) and Chanson (2001).

It is the purpose of this paper to assess critically the effects of free-surface aeration on flow resistance in skimming flows. New air–water flow experiments were performed with channel slopes of 16° and 22°. The results are compared with the re-analysis of existing data (Table 1) and they demonstrate some reduction in flow resistance caused by free-surface aeration, although the basic mechanism differs from smooth-invert chute flows.

2 Experimental investigations

New experiments were conducted at the University of Queensland in a 5-m long, 1-m wide chute (Table 1). Waters were supplied from a large feeding basin leading to a sidewall convergent with a 4.8 : 1 contraction ratio. The test section consisted of

Revision received

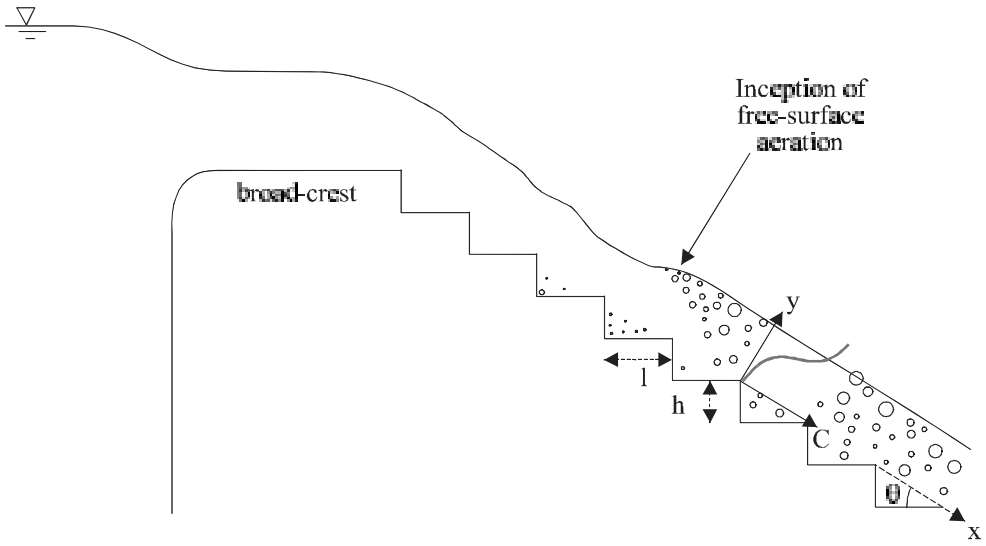

Figure 1 Skimming flow on a stepped chute — Definition sketch.

Table 1 Experimental data on drag reduction in skimming flows

Reference	θ (°)	q_w (m^2/s)	h (m)	Re $V * D_H/\nu_w$	f_e	Instrumentation	Inflow conditions	Remarks
(1)	(2)	(3)	(4)	(5)	(6)	(7)	(8)	(9)
Chamani and Rajaratnam (1999)						SAF conductivity probe	Uncontrolled smooth WES ogee	$W = 0.3$ m
	51.3	0.0725–0.205	0.313–0.125	2.5E × 10^5 –6.0E × 10^5	0.10–0.22			
	59	0.0725–0.205	0.313–0.125	2.5E × 10^5 –5.9E × 10^5	0.12–0.24			
Ohtsu *et al*. (2000)						Optical fibre probe	Uncontrolled broad-crest	$W = 0.4$ m
	55	0.031	0.025	1.1E × 10^5 –1.2E × 10^5	0.11–0.22			
Matos (2000)						SAF conductivity probe	Uncontrolled WES ogee, with smaller first steps built in ogee development	$W = 1$ m
	53.1	0.08–0.20	0.08	3.2E × 10^5 –7.9E × 10^5	0.06–0.10			
Boes (2000)						Optical fibre probe	Pressurized intake (jetbox)	$W = 0.5$ m
	30	0.05–0.38	0.046–0.092	1.8E × 10^5 –1.1E × 10^6	0.09–0.13			
	50	0.065–0.34	0.031–0.092	3.3E × 10^5 –1.1E × 10^6	0.07–0.12			
Present study						Needle-type conductivity probe	Uncontrolled broad-crest	$W = 1$ m
	21.8	0.10–0.18	0.10	$4E \times 10^5$ –7.2E × 10^5	0.07–0.28[a]			
	15.9	0.10–19	0.10	4.3E × 10^5 –7.5E × 10^5	0.11–0.14			
	15.9	0.078	0.05	3.1E × 10^5	0.11			

[a]Full data set in Chanson and Toombes (2001a,b). All flumes were rectangular prismatic channels.

an uncontrolled broad-crest followed by nine 0.1-m high steps or eighteen 0.05-m high steps. Two slopes were investigated: $\theta = 15.9°$ and 21.8° corresponding to step lengths of 0.35 and 0.25 m ($h = 0.1$ m) respectively, and 0.125 m ($h = 0.05$ m, $\theta = 15.9°$). The stepped chute had perspex sidewalls and the flow rate was delivered by a pump controlled with an adjustable frequency AC motor drive.

Air–water flow properties were measured using conductivity probes: a single-tip probe with 0.35 mm sensor size and a double-tip probe with a 25-micron sensor size. The probes were excited by an air bubble detector (AS25240) and the probe signal was scanned at 5–40 kHz for 20–180 s. The translation of the probes in the direction normal to the channel invert was controlled by a fine adjustment travelling mechanism. The error on the normal position of the probe was less than $\Delta y < 0.1$ mm. Flow visualizations were conducted with digital video-camera and high-speed still photographs. Further details were reported in Chanson and Toombes (2001a).

2.1 Flow resistance calculations

For $h = 0.1$ m, the flow was gradually varied at the downstream end of the chute. The equivalent Darcy friction factor was deduced from the friction slope S_f:

$$f_e = \frac{8g}{q_w^2}\left(\int_{y=0}^{y=Y_{90}}(1-C)\mathrm{d}y\right)^3 S_f \quad (1)$$

where f_e is the pseudo Darcy friction factor for air–water flow, g is the gravity acceleration, q_w is the water discharge per unit width, C is the air concentration, y is the distance normal to the pseudo-bottom formed by the step edges, Y_{90} is the characteristic distance where $C = 90\%$, S_f is the friction slope ($S_f = -\partial H/\partial x$), H is the total head and x is the distance in the flow direction. The total head and the friction factor were calculated based upon the air–water flow properties measured at step edges (e.g. Fig. 2). At uniform equilibrium (e.g. $h = 0.05$ m, $\theta = 15.9°$), the flow resistance was calculated using the momentum equation:

$$f_e = \frac{8g}{q_w^2}\left(\int_{y=0}^{y=Y_{90}}(1-C)\mathrm{d}y\right)^3 \sin\theta \quad (2)$$

where θ is the slope of the pseudo-invert formed by the step edges (e.g. Chanson *et al.*, 2000).

The results were compared with the re-analysis of detailed air concentration measurements in skimming flows (Table 1). Experimental data obtained in gradually varied flows and in normal flows were computed using Eqs. (1) and (2), respectively.

3 Experimental results

Air–water flow measurements showed smooth, continuous distributions of air concentrations and air–water velocity from the pseudo-bottom formed by the step edges ($y = 0$) up to the upper flow region. Figure 2 presents a series of results obtained on the 16° cascade ($h = 0.1$ m), where the black and white symbols are respectively, air concentration and air–water velocity data measured at step edges, and the cross symbols are air concentration data measured at half-distances between step edges. In Fig. 2, the air concentration data at step edges are compared with a theoretical model of the air bubble diffusion (Chanson and Toombes, 2001a), while the velocity data are compared with a one-sixth power law for $y/Y_{90} < 1$.

For all experiments, there was a marked change in air concentration profiles measured at step edges and above the recirculating cavities. Greater flow aeration was observed consistently between

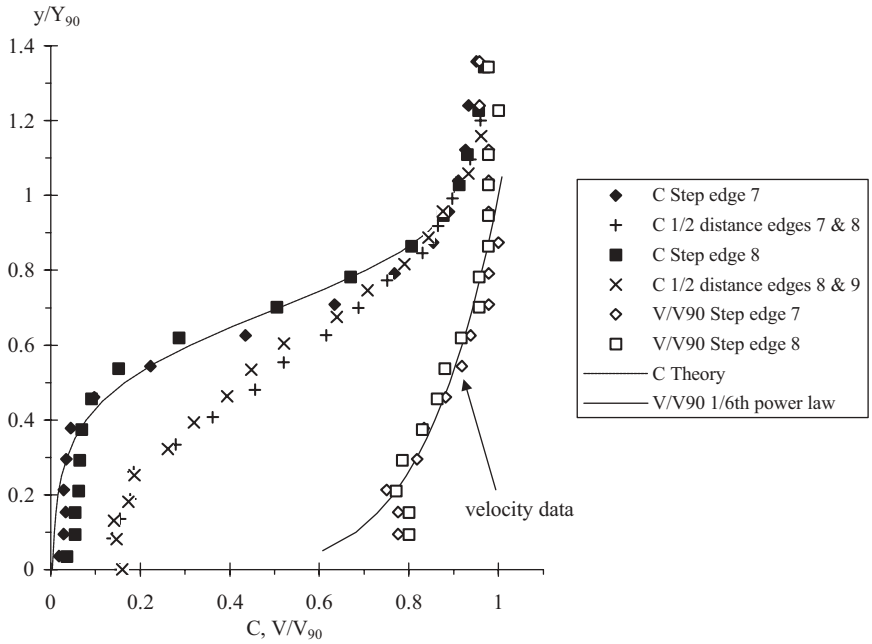

Figure 2 Air concentration and dimensionless distributions in skimming flows at step edges and at half-distances between step edges — $\theta_w = 0.188\,m^2/s$, $h = 0.1$ m, $\theta = 15.9°$ (present study, double-tip probe). Black symbols: air concentration data measured at step edges; white symbols: air–water velocity data measured at step edges; crosses: air concentration data measured at half-distance between step edges.

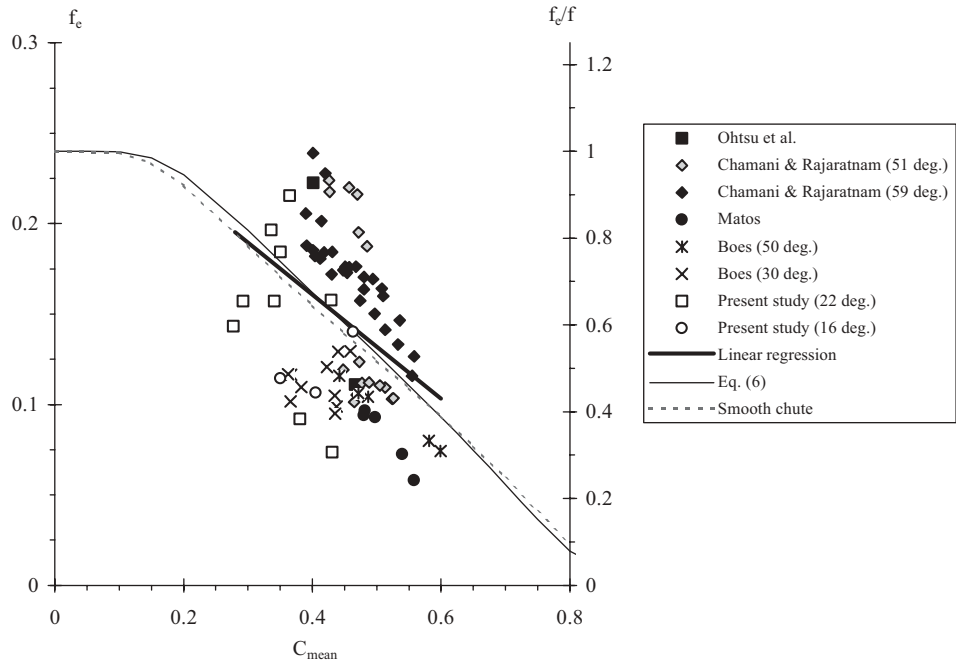

Figure 3 Flow resistance in self-aerated skimming flows. (a) Darcy friction factor f_e as a function of the depth-averaged air concentration C_{mean}; (b) relative flow resistance f_e/f as a function of the depth-averaged air concentration C_{mean}.

step edges (Fig. 2, cross symbols) than at adjacent step edges (Fig. 2, black symbols), in particular in the fluid layers next to the recirculation cavity (i.e. $y/Y_{90} < 0.3$–0.5). Similar observations were reported by Boes (2000) and Matos *et al.* (2001). It is believed that cavity aeration is caused by air bubbles trapped in the core of recirculating vortices by inertial forces (e.g. Tooby *et al.*, 1977). Vortex trapping of bubbles leads to higher air content in the cavity flow and in the mixing layers downstream of the step edges (Figs 1 and 5).

Flow resistance data are summarized in Fig. 3, showing the Darcy friction factor f_e as a function of the mean air concentration C_{mean} measured at step edges and defined as:

$$C_{mean} = \frac{1}{Y_{90}} \int_{y=0}^{Y_{90}} C dy \quad (3)$$

Experimental results (white symbols) are compared with the reanalysis of detailed air–water flow measurements (black and cross symbols) (Table 1). First, the results show a broad scatter which may be caused by differences in slope, instrumentation and inflow conditions (see Table 1, columns 2, 7 and 8, respectively). For example, Boes (2000) and Ohtsu *et al.* (2000) used optical fibre probes; Chamani and Rajaratnam (1999) and Matos (2000) used a SAF electrical probe, while the present study used a smaller design of resistivity probe (needle-probe design). Chanson and Toombes (2001b) discussed specifically the effect of inflow conditions on skimming flow resistance arguing that recirculation cavity instabilities might be related to the inflow conditions. Their analysis suggested greater flow resistance with uncontrolled broad-crest intake than with pressurized inflow.

Second, the data exhibit an overall trend which is correlated by:

$$f_e = 0.276 - 0.288 C_{mean}, \qquad 0.28 < C_{mean} < 0.60 \quad (4)$$

with a correlation coefficient of 0.392. Equation (4) suggests a decrease in friction factor f_e with increasing mean air content in skimming flows. The trend is basically independent of the pseudo-slope of the invert.

3.1 Comparison with monophase flows

Flow resistance in monophase flows above large roughness is presented in Fig. 4 as a function of the relative roughness height k_S/D_H where k_S is the roughness height and D_H is the hydraulic diameter. The experimental data correspond to relative roughness height similar to relative step cavity height $h \cos\theta/D_H$ for stepped chute flows. Experimental data obtained in mountain rivers and prototype rockfill channels (white symbols) are compared with clear-water flows above triangular roughness elements (cross symbols).

In monophase flows, Wygnanski and Fiedler (1970) observed experimentally that the maximum shear stress in mixing layers above rectangular cavities is independent of the distance from the singularity and their data yielded $f = 0.18$. For rectangular cavity flows also, Haugen and Dhanak (1966) and Kistler and Tan (1967) observed similar results. Chanson *et al.* (2002) developed an analytical estimate of the maximum shear stress in the mixing layer (Fig. 5). Their development yielded:

$$f = \frac{2}{\sqrt{\pi} K} \quad (5)$$

where $1/K$ is a dimensionless rate of expansion of the shear layer with $K \approx 6$ in air–water shear flows yielding $f \sim 0.2$. A comparison between all these observations and measured flow resistance in air–water skimming flows is presented in Fig. 4, where equivalent friction factors in monophase flows over large roughness ranged between 0.1 and 0.3. The result suggests lower pseudo-friction factors in air–water skimming flows (Fig. 4,

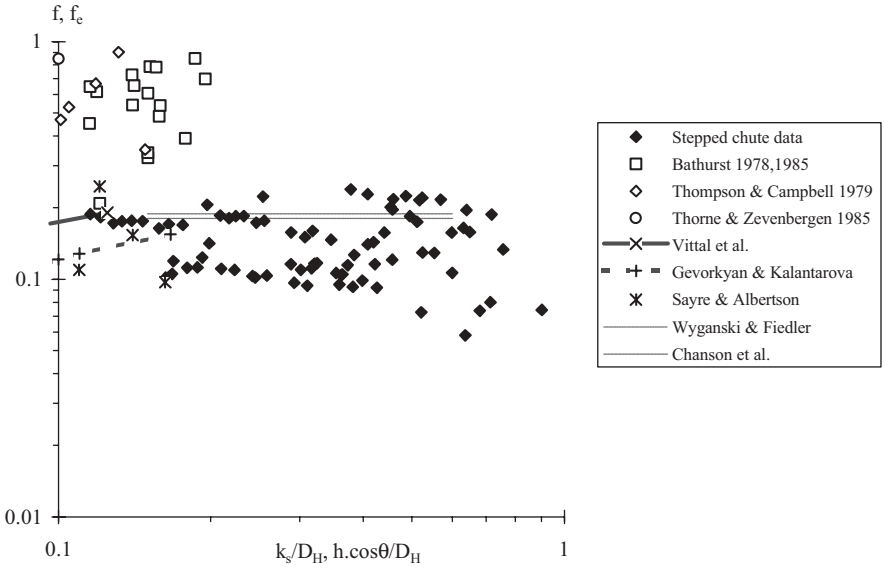

Figure 4 Flow resistance with large roughness elements — comparison between rockfill channel data (white symbols), flows past large roughness elements (cross symbols) and self-aerated skimming flows (black symbols).

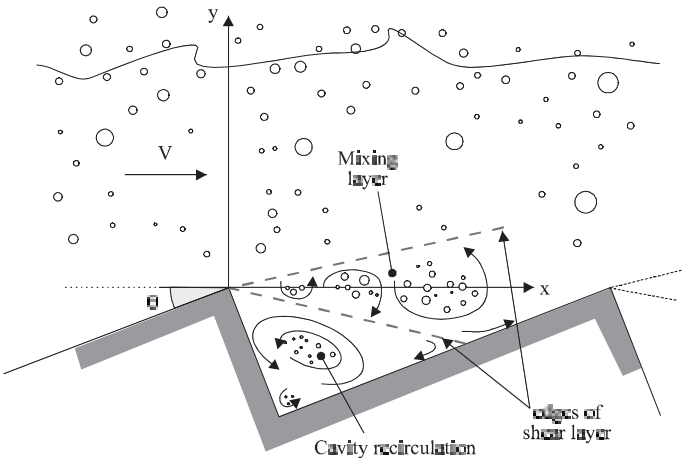

Figure 5 Sketch of interactions between developing mixing layer and entrained air bubbles.

black symbols) and the reduction in flow resistance might be correlated by:

$$\frac{f_e}{f} = 0.5 \times \left[1 + \tanh\left(0.71 \times \frac{0.52 - C_{mean}}{C_{mean}(1 - C_{mean})}\right)\right] \quad (6)$$

where tanh is the hyperbolic tangent function and f is an estimate of form drag friction factor in monophase flow. Equation (6) is shown in Fig. 3 (right vertical axis) for $f = 0.24$ (correlation coefficient of 0.395). It is a rough estimate that does satisfy basic boundary conditions: i.e. $f_e/f = 1$ in clear-water flow ($C_{mean} = 0$) and f_e/f negligible in air flow ($C_{mean} = 1$). Despite some scatter, the trend confirms Chanson's (1993) assumption that free-surface aeration induces a drag reduction process in skimming flows above a stepped spillway.

4 Discussion

On smooth-invert chutes, the presence of air within turbulent boundary layers reduces the shear stress between flow layers (Wood, 1983; Chanson, 1994). An estimate of the drag reduction is:

$$\frac{f_e}{f} = 0.5 \times \left[1 + \tanh\left(0.628 \times \frac{0.514 - C_{mean}}{C_{mean}(1 - C_{mean})}\right)\right] \quad (7)$$

Equation (7) characterizes the reduction in skin friction associated with air entrainment causing a thickening of the "viscous" sublayer (Chanson, 1994). It is plotted in Fig. 3. The trend is very close to Eq. (6) although the drag reduction mechanism is entirely different.

In skimming flows, separation occurs at each step edge and a shear layer develops with cavity recirculation beneath (Fig. 5). It is believed that drag reduction results from interactions between entrained bubbles and developing mixing layer. Small air bubbles tend to resist stretching in the shear layer and this leads to some vortex inhibition. Hydrodynamic interactions between bubbles affect their orientation in the flow and might play a key role in reducing the instability of the flow as with fibre addition in water flows (e.g. Azaiez, 2000). Riediger (1989) and Warholic *et al.* (2001) visualized interactions between particles and turbulent structures in turbulent shear flows of dilute polymer solutions. They showed the existence of large-scale turbulent structures and a drastic reduction in number of small-scale eddies, hence a reduction in momentum exchange across the mixing layers. In skimming flows, such a result yields a reduction in flow resistance according to Eq. (5).

In summary, the strong aeration of both recirculating cavity and mixing layer, illustrated in Fig. 2, play a major role in the drag reduction process.

4.1 Design application

Design engineers must take into account flow aeration to estimate the flow properties used to calculate the flow velocity, and to dimension chute sidewall heights and downstream energy

dissipators. The residual head equals:

$$H_{res} = d\cos\theta + \frac{q_w^2}{2gd^2} \quad (8)$$

where d is the equivalent clear-water depth [i.e. $d = (1 - C_{mean})Y_{90}$]. In uniform equilibrium flows, the clear water depth equals:

$$\frac{d}{d_c} = \sqrt[3]{\frac{f_e}{8\sin\theta}} \quad (9)$$

for a wide channel, where d_c is the critical depth, the Darcy friction factor f_e is estimated using Eq. (6) and $f = 0.24$ for flat horizontal steps. In Eq. (6), the mean air content may be estimated as in smooth-chute flows (Wood, 1983; Chanson, 1993, 2001). In gradually varied flows, the clear-water depth must be deduced from the integration of the energy equation in which the friction slope is estimated as:

$$S_f = \sqrt{\frac{f_e}{8}} \times \frac{q_w^2}{gd^3} \quad (10)$$

for a wide channel. Alternately a simplified method may be used, as developed by Chanson (2001, pp. 174–175).

5 Conclusion

Detailed air–water flow measurements in skimming flows down stepped chutes were performed and the results are compared with the re-analysis of air–water flow studies. Overall the results show a decrease in air–water flow resistance with increasing mean air content. Experimental results are compared with experimental data in monophase flows and this suggests some drag reduction caused by free-surface aeration. Although the trend is close to a previous result obtained in smooth-invert chute flows, the mechanism of drag reduction is completely different. In skimming flow, drag reduction is caused by interactions between entrained air bubbles and developing mixing layers. The process is affected by a strong cavity aeration induced by inertial effect (Fig. 2).

The present results are limited to flat horizontal steps, chute slopes between 16° and 60°, and mean air contents between 0.25 and 0.65. Further experimental work is required to gain a clearer understanding of the interactions between entrained air and mixing layers for a wider range of flow conditions.

Acknowledgments

The writer acknowledges the assistance of Dr Y. Yasuda (Nihon University), Mr C. Gonzalez and Dr L. Toombes (University of Queensland). He thanks Dr J. Matos, IST-Lisbon and Dr Y. Yasuda for providing their experimental data.

Notation

C = air concentration defined as the volume of air per unit volume (note: also called void fraction)
C_{mean} = depth averaged air concentration defined as: $(1 - Y_{90})C_{mean} = d$
D_H = hydraulic diameter (m)
d = equivalent clear-water depth (m) defined as: $d = \int_0^{Y_{90}} (1 - C)\mathrm{d}y$
d_c = critical depth
f = Darcy friction factor for clear-water (non-aerated) flow
f_e = Darcy friction factor for air–water flow
g = gravity constant (m/s^2) or acceleration of gravity
H = total head (m)
H_{res} = residual head (m) at the downstream end of the chute
h = height of steps (m) (measured vertically)
K = inverse of the spreading rate of a turbulent shear layer
q_w = water discharge per unit width (m^2/s)
Re = Reynolds number defined as: Re $= V D_H/\nu_w$
S_f = friction slope: $S_f = -\partial H/\partial x$
V = clear-water flow velocity (m/s): $V = q_w/d = q_w/\int_0^{Y_{90}} (1 - C)\mathrm{d}y$
W = channel width (m)
x = longitudinal distance (m) measured in the flow direction
Y_{90} = characteristic depth (m) where the air concentration is 90%
y = distance (m) from the pseudo-bottom (formed by the step edges) measured perpendicular to the flow direction

Greek symbols
ν_w = kinematic viscosity (m^2/s) of water
θ = channel slope.

References

1. AZAIEZ, J. (2000). "Reduction of Free Shear Flows Instability: Effects of Polymer versus Fibre Additives." *J. Non-Newtonian Fluid Mec.* 91, 233–254.
2. BATHIRST, J.C. (1978). "Flow Resistance of Large-Scale Roughness." *J. Hydr. Div. ASCE* 104(HY12), 1587–1603.
3. BATHIRST, J.C. (1985). "Flow Resistance Estimation in Mountain Rivers." *J, Hydr. Engrg. ASCE* 111(4), 625–643.
4. BOES, R.M. (2000). "Zweiphasenströmung und Energieumsetzung auf Grosskaskaden." PhD Thesis, ETHZürich, Switzerland.
5. CHAMANI, M.R. and RAJARATNAM, N. (1999). "Characteristics of Skimming Flow over Stepped Spillways." *J. Hydr. Engrg. ASCE* 125(4), 361–368.
6. CHANSON, H. (1993). "Stepped Spillway Flows and Air Entrainment." *Can. J. Civil Engrg.* 20(3), 422–435.
7. CHANSON, H. (1994) "Drag Reduction in Open Channel Flow by Aeration and Suspended Load." *J. Hydr. Res.* IAHR, 32(1) 87–101.
8. CHANSON, H. (2001). *The Hydraulics of Stepped Chutes and Spillways*. Swets & Zeitlinger, Lisse, The Netherlands.
9. CHANSON, H. and TOOMBES, L. (2001a). "Strong Interactions between Free-Surface Aeration and Turbulence down a Staircase Channel." In: *Proceedings of the 14th Australasian Fluid Mechanics Conference*, Adelaide, Australia, pp. 841–844.

10. CHANSON, H. and TOOMBES, L. (2001b). "Experimental Investigations of Air Entrainment in Transition and Skimming Flows down a Stepped Chute. Application to Embankment Overflow Stepped Spillways." Research Report CE 158, Department of Civil Engineering, University of Queensland, Brisbane, Australia, July, 74 pp.
11. CHANSON, H., YASUDA, Y. and OHTSU, I. (2000). "Flow Resistance in Skimming Flow: a Critical Review." In: Minor, H.E. and Hager, W.H. (eds), *International Workshop on Hydraulics of Stepped Spillways*, Zürich, Switzerland. Balkema Publ., pp. 95–102.
12. CHANSON, H., YASUDA, Y. and OHTSU, I. (2002). "Flow Resistance in Skimming Flow and it Modelling." *Can. J. Civil Engrg.* 29(6), 809–819.
13. GEVORKYAN, S.G. and KALANTAROVA, Z.K. (1992). "Design of Tsunami-Protective Embankments with a Complex Front Surface." *Gidrotekhnicheskoe Stroitel'stvo*, No. 5, May, pp. 19–21 (in Russian) (Translated in Hydrotechnical Construction, 1992, Plenum Publ., pp. 286–290).
14. HAUGEN, H.L. and DHANAK, A.M. (1966). "Momentum Transfer in Turbulent Separated Flow past a Rectangular Cavity." *J. Appl. Mech. Trans. ASME* 641–464.
15. KISTLER, A.L. and TAN, F.C. (1967). "Some Properties of Turbulent Separated Flows." *Phys. Fluids* 10(9), S165–S173.
16. MATOS, J. (2000). "Hydraulic Design of Stepped Spillways over RCC Dams." In: MINOR, H.E. and HAGER, W.H. (eds), *International Workshop on Hydraulics of Stepped Spillways*, Zürich, Switzerland, Balkema Publ., pp. 187–194.
17. MATOS, J., YASUDA, Y. and CHANSON, H. (2001). "Interaction between Free-surface Aeration and Cavity Recirculation in Skimming Flows down Stepped Chutes." In: *Proceedings of the 29th IAHR Congress*, Beijing, China, Theme D, Sub-theme D5–24.
18. OHTSU, I., YASUDA, Y. and TAKAHASHI, M. (2000). "Characteristics of Skimming Flow over Stepped Spillways. Discussion." *J. Hydr. Engrg. ASCE* 126(11), 869–871.
19. PEYRAS, L., ROYET, P. and DEGOUTTE, G. (1992). "Flow and Energy Dissipation over Stepped Gabion Weirs." *J. Hydr. Engrg. ASCE* 118(5), 707–717.
20. RAJARATNAM, N. (1990). "Skimming Flow in Stepped Spillways." *J. Hydr. Engrg. ASCE* 116(4), 587–591.
21. RIEDIGER, S. (1989). "Influence of Drag Reducing Additives on a Plane Mixing Layer." In: *Proceedings of the 4th International Conference on Drag Reduction*, Davos, Switzerland. Ellis Horwood Publ., Chichester, UK, No. 10.4, pp. 303–310.
22. SAYRE, W.W. and ALBERTSON, M.L. (1963). "Roughness Spacing in Rigid Open Channels." *Trans. ASCE* 128, 343–372; (Discussion: 128, 372–427).
23. THOMPSON, S.M. and CAMPBELL, P.L. (1979). "Hydraulics of a Large Channel Paved with Boulders." *J. Hydr. Res. IAHR* 17(4), 341–354.
24. THORNE, C.R. and ZEVENBERGEN, L.W. (1985). "Estimating Velocity in Mountain Rivers." *J. Hydr. Engrg. ASCE* 111(4), 612–624.
25. TOOBY, P.F., WICK, G.L. and ISACS, J.D. (1977). "The Motion of a Small Sphere in a Rotating Velocity Field: A Possible Mechanism for Suspending Particles in Turbulence." *J. Geophy. Res.*, 82(15), 2096–2100.
26. VITTAL, N., RAGA RAJU, K.G. and GARDE, R.J. (1977). "Resistance of Two Dimensional Triangular Roughness." *J. Hydr. Res. IAHR* 15(1), 19–36.
27. WYGNANSKI, I. and FIEDLER, H.E. (1970). "The Two-Dimensional Mixing Region." *J. Fluid Mech.* 41, 327–361.
28. WARHOLIC, M.D., HEIST, D.K., KATCHER, M. and HANRATTY, T.J. (2001). "A Study with Particle-Image Velocimetry of the Influence of Drag-Reducing Polymers on the Structure of Turbulence." *Exp. Fluids* 31(5), 474–483.
29. WOOD, I.R. (1983). "Uniform Region of Self-Aerated Flow." *J. Hydr. Engrg. ASCE* 109(3), 447–461.